

Manuscript Number: STOTEN-D-15-02388R3

Title: Association of environmental benzo[a]pyrene exposure and DNA methylation alterations in Hepatocellular Carcinoma: a Chinese case-control study

Article Type: Research Paper

Keywords: B[a]P; Case control study; DNA methylation; Epigenetic; GSTP; Hepatocellular carcinoma

Corresponding Author: Prof. Heqing Shen, Ph.D

Corresponding Author's Institution: Institute of Urban Environment, Chinese Academy of Sciences

First Author: Meiping Tian

Order of Authors: Meiping Tian; Heqing Shen, Ph.D

Abstract: Epidemiological studies implicate environmental risk factors and epigenetic alterations in the multistage process of hepatocellular carcinoma (HCC) development. However, associations between environmental factors and DNA methylation of tumour suppressor genes (TSGs) in HCC development remain ambiguous. Understanding how possible interactions influence risk may provide insights into the complexity of hepatocarcinogenesis. For this study, blood samples were collected from HCC patients (n=90) and healthy volunteers (n=99) from Xiamen (China) and data for selected environmental risk factors [e.g., benzo[a]pyrene (B[a]P), hepatitis B or C virus (HBV or HCV) infection, smoking and alcohol consumption] were recorded; factors identified as significantly higher ($P < 0.05$) amongst case subjects compared to controls were identified. In order to assess associations for epigenetic alterations and HCC risk factors, serum DNA methylation of TSGs was quantified using high-resolution melting (HRM) analysis. Our results clearly indicate elevated methylation patterns for detoxification gene [glutathione-S-transferase Pi (GSTP)] promoter regions in cases compared to control subjects. Additionally, GSTP promoter hypermethylation and B[a]P diol epoxide-albumin (BPDE-Alb) were positively correlated with HCC incidence. Our epidemiological and in vitro cell model studies indicated that GSTP promoter DNA methylation regulates this gene's expression. Moreover, GSTP also plays an important role in B[a]P detoxification and potential protective role against B[a]P-induced liver cell toxicity and hepatocarcinogenesis.

Response to Reviewers: Reviewers/Editor comments:

The submission still suffers from spelling, grammar, and flow issues around language. Please have it reviewed and revised by a native English speaker.

Response: We really appreciate the comments and suggestion from editor and reviewers. We have invited Prof. Frank Martin reviewed and revised

the manuscript carefully and made the related revision in the revised manuscript (highlighted in yellow).

1 1 **Association of environmental benzo[a]pyrene exposure and DNA methylation**
2
3 2 **alterations in hepatocellular carcinoma: a Chinese case-control study**

4
5
6 3 Meiping Tian¹, Benhua Zhao², Jie Zhang¹, Francis L. Martin³, Qingyu Huang¹,
7
8 4 Liangpo Liu¹, Heqing Shen^{1*}

9
10
11 5 *¹Institute of Urban Environment, Chinese Academy of Sciences, Key Lab of Urban*
12
13 6 *Environment and Health, Xiamen, 361021, PR China*

14
15
16 7 *²School of Public Health, Xiamen University, Xiamen, 361102, PR China*

17
18
19 8 *³Centre for Biophotonics, LEC, Lancaster University, Lancaster LA1 4YQ, UK*

20
21
22
23 9

24
25
26 10

27
28
29 11

30
31
32 12

33
34
35 13

36
37 14 ***Corresponding author details:** 1799 Jimei Road, Xiamen 361021, PR China;

38
39 15 Tel.: +86-592-6190771; Fax: +86-592-6190771; E-mail: hqshen@iue.ac.cn

40
41
42 16

43
44
45 17

46
47
48 18

49
50
51 19

52
53
54 20

55
56
57 21

58
59 22

60
61
62
63
64
65

23 **Abstract**

24 Epidemiological studies implicate environmental risk factors and epigenetic
25 alterations in the multistage process of hepatocellular carcinoma (HCC) development.
26 However, associations between environmental factors and DNA methylation of
27 tumour suppressor genes (TSGs) in HCC development remain ambiguous.
28 Understanding how possible interactions influence risk may provide insights into the
29 complexity of hepato-carcinogenesis. For this study, blood samples were collected
30 from HCC patients ($n=90$) and healthy volunteers ($n=99$) from Xiamen (China) and
31 data for selected environmental risk factors [*e.g.*, benzo[*a*]pyrene (B[*a*]P), hepatitis B
32 or C virus (HBV or HCV) infection, smoking and alcohol consumption] were
33 recorded; factors identified as significantly higher ($P < 0.05$) amongst case subjects
34 compared to controls were identified. In order to assess associations for epigenetic
35 alterations and HCC risk factors, serum DNA methylation of TSGs was quantified
36 using high-resolution melting (HRM) analysis. Our results clearly indicate elevated
37 methylation patterns for detoxification gene [glutathione-*S*-transferase Pi (*GSTP*)]
38 promoter regions in cases compared to control subjects. Additionally, *GSTP* promoter
39 hypermethylation and B[*a*]P diol epoxide-albumin (BPDE-Alb) were positively
40 correlated with HCC incidence. Our epidemiological and *in vitro* cell model studies
41 indicated that *GSTP* promoter DNA methylation regulates this gene's expression.
42 Moreover, *GSTP* also plays an important role in B[*a*]P detoxification and potential
43 protective role against B[*a*]P-induced liver cell toxicity and hepato-carcinogenesis.

44
45 **Keywords:** B[*a*]P; Case control study; DNA methylation; Epigenetic; *GSTP*;
46 Hepatocellular carcinoma

1
2
3
4
5
6
7
8
9
10
11
12
13
14
15
16
17
18
19
20
21
22
23
24
25
26
27
28
29
30
31
32
33
34
35
36
37
38
39
40
41
42
43
44
45
46
47
48 **1. Introduction**

49 Hepatocellular carcinoma (HCC) is the 4th most common cancer worldwide and
50 a major cause of cancer-related deaths, especially in sub-Saharan countries, Southeast
51 Asia and China. Incidence rates of HCC in China have increased to 30/100,000; this
52 equates to approximately 55% of total worldwide cases (Chen et al., 2005, and Parkin
53 et al., 2002). Epidemiological studies suggest that both environmental risk factors and
54 genetic alterations are associated with HCC development (Chen et al., 2002, Johnson
55 et al., 2010 and Lambert et al., 2011), but the precise underlying mechanism(s)
56 leading to hepato-carcinogenesis remain unclear.

57 HCC is considered as mostly an environmental-related cancer, with both viral
58 and chemical carcinogen components implicated in its multistage process (Zhao et al.
59 2010). Hepatitis B virus (HBV) or hepatitis C virus (HCV) infection is considered a
60 major risk factor (Lambert et al., 2011). Apart from infection, environmental pollution
61 or unhealthy lifestyle may also provide a direct exposure route to many toxins that
62 destabilize genomic integrity and/or deregulate epigenetic markings. Among many
63 pollutants, benzo[*a*]pyrene (B[*a*]P), a polycyclic aromatic hydrocarbon (PAH), has
64 been reported to occur in the environment as result of incomplete combustion of
65 organic materials. B[*a*]P is a pro-carcinogen and, systemically in humans, can be
66 converted into reactive metabolites [*e.g.*, B[*a*]P diol epoxide (BPDE)] by cytochrome
67 P4501A1 (CYP1A1); such reactive metabolites covalently bind to DNA, potentially
68 causing genomic alterations (Ko et al., 2004). Covalent interaction between BPDE
69 and nucleophilic centres in DNA is thought to be a critical event in the initiation of
70 B[*a*]P-induced tumorigenesis. Hence, B[*a*]P and its cellular metabolite BPDE may

1 71 instigate genomic and epigenomic alterations (Feng et al., 2002 and Tang et al.,
2
3 72 2012).

4
5
6 73 Aberrant DNA methylation is widely documented as an important epigenomic
7
8
9 74 event in the development and progression of many cancers, including HCC (Herceg
10
11 75 2007, Huang et al., 2011, Lambert et al., 2011 and Zhang et al., 2007). Recent studies
12
13
14 76 demonstrate that aberrant DNA methylation of specific TSG promoters (*e.g.*, *APC*,
15
16
17 77 *GSTP*, *P15*, *SOCS-1* and *RASSF1A*) and global genomes have been frequently
18
19
20 78 observed in HCC (Esteller et al., 2001, Lambert et al., 2011 and Yang et al., 2003).
21
22
23 79 Hypermethylation of TSG CpG islands inhibit transcriptional initiation and silence
24
25
26 80 expression of downstream genes; particularly, if detoxification genes are silenced, by
27
28
29 81 allowing intracellular accumulation of toxins, this may facilitate the carcinogenesis
30
31
32 82 process. However, the association between environment pollutants, epigenetic
33
34
35 83 modifications and HCC risk remains unknown. Herein, we investigated a
36
37
38 84 hospital-based case-control cohort resident in the middle of the South East coastline
39
40
41 85 of China, a high HCC incidence belt (Xu et al., 2003). In addition, an *in-vitro* cell
42
43
44 86 model was employed to assess the effects of B[a]P exposure and its association with
45
46
47 87 detoxification gene promoter DNA methylation modifications and HCC development.
48

49

50 89 **2. Materials and methods**

51 52 53 90 *2.1 Samples and clinical characteristics of participants*

54
55
56 91 Peripheral blood samples from newly diagnosed HCC patients ($n=90$) before
57
58
59 92 treatment and healthy volunteers ($n=99$) were obtained from Zhongshan Hospital of
60
61

1 93 Xiamen University, Xiamen Hospital of Traditional Chinese Medicine and the 174th
2
3 94 hospital of the People's Liberation Army. All the HCC cases were clinic patients who
4
5
6 95 were determined by clinical and radiological evaluation not to suffer any other cancer
7
8
9 96 types. Written informed consent was obtained from all participants. A structured
10
11
12 97 questionnaire and survey was conducted, as previously described (Zhao et al., 2010).
13
14 98 The structured questionnaire included participant demographics (*e.g.*, sex, age, height,
15
16
17 99 body weight, income, employment status and occupational history); additional
18
19
20 100 information including history of cigarette smoking, alcohol consumption, disease,
21
22
23 101 diabetes mellitus, physical activity and viral infection (HBV, HCV) were collected
24
25
26 102 from the participants or clinical documents with the permission of related
27
28
29 103 stakeholders (Niu et al., 2010 and Zhao et al., 2012).

30 104 2. 2 Measurement of the serum benzo[a]pyrene diol epoxide-albumin (BPDE-Alb)

31
32
33
34 105 Serum BPDE-Alb adducts, a widely used biomarker for B[a]P exposure, were
35
36
37 106 measured using reverse-phase high performance liquid chromatography, as previously
38
39
40 107 described (Islam et al., 1999). In brief, 4 mL blood from participants were collected
41
42
43 108 into Na-heparin tubes, and plasma separated by centrifugation at 1200×g for 10 min.
44
45
46 109 Plasma was obtained and precipitated with one volume of saturated ammonium
47
48
49 110 sulfate overnight, followed by 15 min centrifugation at 1200×g. To 1 mL of
50
51
52 111 supernatant, 10 µL of concentrated acetic acid was added. The solution was left at
53
54
55 112 room temperature overnight followed by 15 min centrifugation at 1200×g. The
56
57
58 113 precipitated albumin, was washed with 4 mL acetone:ethylacetate (1:1) to remove
59
60
61 114 unbound B[a]P metabolites. The precipitate was air-dried at room temperature and

1 115 solubilized in 900 μ L of 10 mM Tris-HCl/1.0 mM EDTA (pH 8.0); the protein
2
3 116 concentration was then determined using the protein quantitative kit (Bio-Rad
4
5
6 117 Laboratories, USA). To 900 μ L albumin was added 100 μ l of 1 M HCl, and this
7
8
9 118 solution was incubated at 90°C for 3 h. Water and methanol were added to a final
10
11
12 119 volume of 5 mL, resulting in a 10% methanol solution. This solution was applied to
13
14
15 120 pre-conditioned (5 ml methanol followed by 10 mL water) Sep-Pak C₁₈ cartridges
16
17 121 (Millipore, Milford, MA) followed by 10 ml washing with water and elution with 5
18
19
20 122 ml of methanol. The eluent was evaporated at 45°C under a nitrogen stream and
21
22
23 123 re-solubilized in 500 μ L of 10% methanol. The samples were stored at -20°C until
24
25
26 124 analysis. Post-hydrolysis, the samples were analyzed with HPLC. For each sample
27
28
29 125 200 μ L was injected. The separation was performed on a Nova-Pak C₁₈ 3.9 \times 150 mm
30
31 126 column (Waters, Milford, USA) with a flow rate of 1.0 mL/min within a Waters LC
32
33
34 127 system (Waters, Milford, USA), equipped with a LC fluorescence detector. The
35
36
37 128 excitation wavelength was 341 nm and the emission was measured at 381 nm.
38
39 129 B[a]P-tetrahydrotetrol was separated by a linear gradient of methanol and water, 30%
40
41
42 130 methanol to 100% methanol in 17 min, 8 min at 100% methanol and then 10 min at
43
44
45 131 30% methanol before the next injection.

132 2.3 Treatment of cell lines with B[a]P

133 To investigate the association between *GSTP* promoter region methylation
134 status and *GSTP* expression, normal immortal human liver (L02) and lung
135 adenocarcinoma (A549) cell lines were selected as *in vitro* models. Both L02 and
136 A549 cell lines were obtained from the Cell Bank of the Chinese Academy of

1 137 Sciences (Shanghai, China) where they were characterized by mycoplasma detection,
2
3 138 immunoperoxidase staining, DNA profiling and cell viability tests. Cell lines were
4
5
6 139 immediately expanded and frozen so they could be restarted every 4 to 5 months
7
8
9 140 from a frozen vial of the same batch of cells. Both cell lines were cultured in DMEM
10
11 141 high-glucose medium (Hyclone, USA). Medium were supplemented with 10% FBS
12
13 142 (Hyclone, USA), 100 unit/mL penicillin and 100 unit/mL streptomycin. L02 and
14
15 143 A549 cells were collected for *GSTP* promoter methylation status analysis and *GSTP*
16
17 144 mRNA expression. A549 cells were employed as a methylation analysis control.
18
19
20
21

22 145 Toward B[a]P exposure experiments, L02 cells were exposed to 0.1, 1 or 10
23
24 146 nM B[a]P (Sigma-Aldrich, St. Louis, Mo) or DMSO alone (vehicle control).
25
26
27 147 Meanwhile, in order to explore the *GSTP* detoxification in B[a]P exposure, L02-cell
28
29 148 *GSTP* promoter regions were de-methylated and gene expression restored with 5 μ M
30
31 149 5-aza-2'-deoxycytidine (DAC) for 2 days treatment prior to exposure to 0.1, 1 or 10
32
33 150 nM B[a]P or DMSO alone (vehicle control). After three days incubation, all cells
34
35
36 151 were harvested and used for DNA or RNA analyses.
37
38
39
40
41

42 152 *2.4 Serum cell-free and cultured cell DNA extraction, and bisulfite treatment*

43

44 153 To remove additional cellular nucleic acids attached to cell debris, aspirated
45
46 154 serum samples were centrifuged at 16,000 \times g for an additional 10 min at 4°C before
47
48 155 DNA extraction. Cell-free DNA (*i.e.*, circulating free) in the serum of participants was
49
50
51 156 extracted using the QIAamp DNA minikit (Qiagen, Hilden, Germany), according to
52
53 157 manufacturer's instructions. Approximately, 200 ng DNA isolated from serum was
54
55
56 158 subjected to sodium bisulfite using the EZ DNA Methylation Kit (Zymo Research,
57
58
59
60
61
62
63
64
65

1 159 Orange, CA, USA), according to manufacturer's instructions; unmethylated cytosines
2
3 160 are converted to uracil whereas methylated cytosines remain unchanged during the
4
5
6 161 reaction. The modified DNA was eluted in elution buffer and used for quantification
7
8
9 162 of DNA methylation.

10 11 163 *2.5 Quantitative DNA methylation measurement*

12
13
14 164 High-resolution melting (HRM) analysis was applied to quantitatively measure
15
16
17 165 the methylation status of *GSTP* promoter regions. Herein, whole genome PCR
18
19
20 166 amplification of monoclonal plasmid from bisulfite-modified CpGenome Universal
21
22
23 167 Methylated DNA (Chemicon, Millipore, Billerica, MA, USA) and genomic DNA
24
25
26 168 from peripheral blood mononuclear cells of normal individuals were selected as
27
28
29 169 methylation and unmethylation controls, respectively. Both of the control plasmids
30
31
32 170 were confirmed by Sanger sequencing before performing an experiment. Methylation
33
34
35 171 standards were constructed by diluting 100% methylated control plasmid in a pool of
36
37
38 172 unmethylated control plasmid at 100%, 75%, 50%, 25%, 10%, 5% and 0% ratios.
39
40
41 173 PCR amplification and HRM analyses were performed on the *LC 480*, as adapted
42
43
44 174 from a published protocol (Roche Applied Science, Germany). Primers used for HRM
45
46
47 175 analysis are shown in Table 1. PCR was performed in a final 20 μ L volume
48
49
50 176 containing: 1 \times ZymoTaq Premix (Zymo, USA), 250 nM of each primer, 2.5 mM
51
52
53 177 *SYTO-9* dye (Invitrogen, Carlsbad, USA) and 10 ng bisulfite-treated DNA template.
54
55
56 178 The cycling conditions started with one cycle at 95°C for 10 min, followed by 60
57
58
59 179 cycles at 95°C for 20 sec each, a touch-down at 64°C to 58°C for 20 sec (1°C/cycle),
60
61
62 180 72°C for 20 sec, and a HRM step of 95°C for 1 min, 40°C for 1 min, 65°C for 5 sec,

1 181 and continuous to 95°C at 25 acquisitions per 1°C. HRM data was analysed by using
2
3 182 gene scanning software (Roche, Germany), as previously described (Stanzer et al.,
4
5
6 183 2010). The melting curves were processed with normalization and temperature
7
8
9 184 shifting using LightCycler Software. Raw data were exported from the LightCycler
10
11
12 185 and used to generate a standard curve by regression analysis. This standard curve was
13
14
15 186 then used to calculate the methylation levels of samples.

17 187 *2.6 Bisulfite sequencing PCR analysis*

18
19
20 188 The alternative quantitative measure of *GSTP* methylation was conducted by
21
22
23 189 bisulfite sequencing PCR (BSP) (Tian et al., 2012). Genomic DNA was
24
25
26 190 bisulfite-modified before PCR. *GSTP* promoter regions were amplified using the
27
28
29 191 sequencing primer (Table 1). The PCR product containing 38 sites was purified using
30
31
32 192 a Wizard SV Gel and PCR Clean-up System (Promega, USA), and cloned into
33
34
35 193 bacteria using the pMD® 18-T Vector (Takara, Japan). Individual clones were grown
36
37 194 overnight and plasmid DNA was isolated with an E.Z.N.A.TM Plasmid Mini Kit
38
39 195 (Promega, USA) and sequenced. Ten to twelve clones were sequenced per group.
40
41
42 196 Sequence results were analysed online by QUMA (<http://quma.cdb.riken.jp>) (Kumaki
43
44
45 197 et al., 2008).

47 198 *2.7 RNA extraction and RT-PCR*

49
50 199 Total RNA was isolated from each cell lines using the High pure RNA isolation
51
52
53 200 Kit (Roche, Germany), according to the manufacture's protocol. First-stand cDNA
54
55
56 201 synthesis was performed with one microgram total RNA using PrimeScript RT
57
58
59 202 reagent Kit with the gDNA Eraser cDNA synthesis Kit (Takara, Japan) employing six
60
61
62
63
64
65

1 203 random primers and oligo dT primer. RT-PCR was performed using the SYBR Green
2
3 204 Master Mix reagents (Roche, Germany). Glyceraldehyde-3-phosphate dehydrogenase
4
5
6 205 (*GAPDH*) was used as an internal reference gene. Primer sets used for amplification
7
8
9 206 are shown in Table 1.

10 11 207 *2.8 Statistical analysis*

12
13
14 208 Statistical analyses were performed using SPSS 18 (SPSS Inc). Variable
15
16
17 209 distributions were analysed by the nonparametric Mann-Whitney *U*-test for
18
19
20 210 continuous variables and χ^2 -test for categorical variables. Due to the non-normal
21
22
23 211 distribution, Spearman correlation coefficients of BPDE-Alb levels with *GSTP*
24
25
26 212 methylation status were calculated. Unconditional multivariate logistic regression was
27
28
29 213 performed for chemical pollutants, which were significantly ($P < 0.05$) associated with
30
31
32 214 HCC in the univariate analysis. Age, gender, BMI and other important HCC risk
33
34
35 215 factors were adjusted using the likelihood-ratio test. Adjusted odds ratios (AOR) and
36
37
38 216 95% confidence intervals (CI) were calculated by the maximum likelihood approach.
39
40
41 217 The quantity assessment of two factors' interaction was also investigated, as
42
43
44 218 previously described (Källberg et al., 2006 and Zhao et al., 2010).

45 220 **3. Results**

46 47 221 48 49 222 *3.1 Demographics and related information*

50
51 223 Demographic and clinical characteristics of study participants are shown in Table
52
53
54 224 2. HCC cases and corresponding controls were well age-matched (57.8 ± 8.4 y *vs.*
55
56
57 225 57.9 ± 8.8 y; $P = 0.96$). The case cohort contained a higher proportion of male subjects,
58
59
60 226 and their body mass index (BMI) levels were lower than the controls (21.2 ± 2.8 *vs.*

1 227 22.4 ± 3.6; $P = 0.01$). Smoking and alcohol consumption subjects were higher among
2
3 228 the cases as compared to controls. The incidence of HBV and HCV was markedly
4
5
6 229 higher in cases than in controls (43.3% vs. 9.1% for HBV; 44.4% vs. 21.2% for HCV).
7
8
9 230 The number of liver cirrhosis patients among cases was also higher compared to
10
11 231 controls (Table 2).

12 232 3.2 *GSTP* promoter methylation and *B[a]P* exposure levels

13
14
15
16
17 233 Human *GSTP* promoter region flank (-226 ~ -78) included 17 CpG sites and/or
18
19
20 234 (-226 ~ +84) included 38 CpG sites. To estimate *GSTP* promoter methylation levels,
21
22 235 HRM PCR was performed on serum cell-free DNA. To test the sensitivity of the
23
24
25 236 HRM assays, we used the standard dilution series as described in the Materials and
26
27
28 237 Methods section. The HRM assay can offer sufficient sensitivity to distinguish the
29
30
31 238 heterogeneous methylation pattern. This assay was able to detect 1% methylation
32
33
34 239 DNA in a background of unmethylated DNA. The correlation coefficient was 0.9919
35
36
37 240 (Figure 1). Furthermore, to verify the reliability of the HRM assays on serum DNA,
38
39 241 we performed BSP assays to quantify the levels of methylation accurately. Figure 2
40
41
42 242 demonstrates the concordance of the methylation status by the HRM and BSP assays.
43
44
45 243 We applied HRM for *GSTP* promoter methylation to analyse the $n=90$ HCC and $n=99$
46
47
48 244 normal serum cell-free DNA. The frequency distribution of *GSTP* methylation status
49
50
51 245 was observed as: methylated (exhibited fully methylated peak, Figure 2),
52
53 246 heterogeneous (exhibited only one broad methylated peak, Figure 2) and
54
55
56 247 unmethylated (only exhibited fully unmethylated peak, Figure 2) in cases (42.2%,
57
58
59 248 11.1% and 44.4%) and controls (6.1%, 11.1% and 77.8%), respectively ($P < 0.001$,

1 249 Table 2). The median DNA methylation levels of *GSTP* promoter regions in cases
2
3 250 (1.62%) were significantly higher than those of controls (0) ($P < 0.001$, Table 3).
4
5

6 251 B[a]P exposure levels in cases were significantly higher than those of the control
7
8 252 group (1.79 fmol/mg adduct vs. 1.51 fmol/mg adduct, $P < 0.001$, Table 3). Meanwhile,
9
10 253 we found a positive correlation between *GSTP* methylation and BPDE-Alb levels in
11
12 254 all subjects ($r = 0.13$, $P = 0.04$). Nevertheless, the median BPDE-Alb exposure level in
13
14 255 all methylated subjects (4.35 fmol/mg) was significantly higher than all unmethylated
15
16 256 subjects (1.66 fmol/mg) ($P = 0.02$), while, there was no significance between
17
18 257 heterogeneous subjects (3.22 fmol/mg) and unmethylated subjects (1.66 fmol/mg) (P
19
20 258 $= 0.15$) as well as methylated subjects (4.35 fmol/mg) ($P = 0.82$) (Figure 3).
21
22
23
24
25
26
27

28 259 Logistic regression was applied to investigate possible associations between
29
30 260 *GSTP* promoter methylation and B[a]P exposure. In the stratification interaction
31
32 261 analysis, after adjustment in the models for confounding variables (*i.e.*, age, BMI, sex,
33
34 262 alcohol consumption, smoking, HBV, HCV and liver cirrhosis), there was a stronger
35
36 263 association between BPDE-Alb adduct levels with HCC risk amongst *GSTP*-M/H
37
38 264 subjects, *i.e.*, methylated and heterogeneous. The AOR for *GSTP*-M/H subjects who
39
40 265 exhibited both low and high BPDE-Alb adduct levels were markedly elevated (3.8
41
42 266 with 95% CI 1.3-10.9; 8.4 with 95% CI 2.7-26.6, $P < 0.001$, for trend see Table 4).
43
44
45
46
47
48
49

50 267 3.3 *GSTP* detoxification in B[a]P exposure

51
52

53 268 In the *in vitro* study, we investigated whether *GSTP* silencing is accompanied by
54
55 269 promoter region hypermethylation. Two human cell (A549 and L02) lines were
56
57 270 investigated, and *GSTP* expression was observed both in vehicle control and
58
59
60
61
62
63
64
65

1 271 DAC-treated A549 cells; promoter region DNA was almost unmethylated, even
2
3 272 following DAC treatment (Figure 4). However, *GSTP* is silenced in L02 cells and its
4
5
6 273 promoter is hypermethylated (78.5%). After DAC treatment, *GSTP* expression was
7
8
9 274 restored with a corresponding decrease in promoter region methylation (57.5%)
10
11
12 275 (Figure 4).

13
14 276 To investigate the action of *GSTP* on detoxification in B[a]P exposure, we
15
16
17 277 further examined the differences in responses to low-dose B[a]P treatment between
18
19
20 278 L02 and DAC-exposed L02 cells. The L02 cell *GSTP* promoter region exhibited
21
22
23 279 hypermethylation, and gene expression was silenced. Contrary to this, DAC-exposed
24
25
26 280 L02 cell *GSTP* promoter region hypomethylation was observed; gene expression was
27
28
29 281 significantly induced by B[a]P. However, *GSTP* promoter methylation status was
30
31
32 282 unchanged by B[a]P exposure (Figure 5). Despite differences in cell models, these
33
34
35 283 observations were associated with similar trends in *CYP1A1* expression induced by
36
37
38 284 B[a]P exposure (Figure 6). However, B[a]P exposure significantly induced the
39
40
41 285 detoxification gene (*GSTP*), oxidative stress response gene (*HO-1*), cell cycle
42
43
44 286 regulation gene (*TP53*), DNA methyltransferases genes (*DNMT1*, *DNMT3A* and
45
46
47 287 *DNMT3B*) and DNA mismatch repair genes (*HMLH1* and *HPMS2*) expression in L02
48
49
50 288 cells, while no significance was found in DAC-treated L02 cells (Figure 6).

51 289 52 53 290 **4 Discussion**

54
55 291 This case-control study demonstrates that BPDE-Alb adducts are significantly (*P*
56
57
58 292 <0.05) higher in HCC cases than those of controls. Similarly, the PAH detoxification
59
60
61
62
63
64
65

1 293 gene *GSTP* promoter region is hypermethylated in HCC serum samples. BPDE-Alb
2
3 294 adducts are significantly correlated with *GSTP* methylation levels in this cohort. In
4
5
6 295 addition, risk for HCC development was highest amongst those individuals who
7
8
9 296 exhibited higher levels of BPDE-Alb adducts and *GSTP* hypermethylation. Our cell
10
11
12 297 model experiments also suggest that loss of *GSTP* expression *via* hypermethylation
13
14 298 results in elevated B[a]P-induced genomic and epigenomic toxicity.
15

16 17 299 *4.1 Environmental exposure of PAHs in HCC*

18
19
20 300 PAHs are ubiquitous environmental pollutants and emitted into surrounding
21
22 301 environment (*i.e.*, air, soil, water, etc.) *via* incomplete combustion of coal, oil, gas,
23
24
25 302 wood, other carbon-containing organic materials and/or cigarette smoke. These
26
27
28 303 ultimately result in human (or other organism, *e.g.*, wildlife) exposure through direct
29
30
31 304 (water, diet) or indirect (dust, air) routes (Su et al., 2014 and Wu et al., 2007). B[a]P is
32
33
34 305 the prototypical PAH and categorized as a pro-carcinogen. The tumorigenic effects of
35
36 306 B[a]P are likely mediated *via* metabolic activation by cytochrome P450 enzymes and
37
38
39 307 epoxide hydrolase into the highly reactive electrophilic metabolite, BPDE; this
40
41
42 308 ultimately forms adducts through covalent binding to DNA and/or albumin.
43
44
45 309 PAH-albumin adducts have been used as a sensitive indicator of chronic low-level
46
47
48 310 PAH exposure, due to lack of repair mechanisms for albumin as compared to DNA.
49
50
51 311 PAH-albumin adducts can also reflect different routes of long-term exposure, and may
52
53 312 account for inter-individual differences for uptake, distribution, metabolism, and
54
55
56 313 elimination (Wu et al., 2007). PAH-albumin adducts have also been reported to be
57
58
59 314 associated with increased HCC risk for other Taiwanese and Xiamen (China) cohorts
60
61
62
63
64
65

1 315 (Wu et al., 2007 and Zhao et al., 2010). One potential mechanism for PAHs in
2
3 316 hepato-carcinogenesis is elevated production of oxidative stress. A previous study
4
5
6 317 found PAH-albumin adducts significantly correlated with urinary
7
8
9 318 8-oxo-7,8-dihydro-2'-deoxyguanosine, a predominant form of free radical-induced
10
11
12 319 oxidative lesions (Autrup et al., 1999). In agreement with our previous findings, the
13
14 320 levels of PAH-albumin and PAH-DNA adducts in HCC blood were significantly
15
16
17 321 higher than those in samples from control subjects (Su et al., 2014 and Zhao et al.,
18
19
20 322 2010). However, this study infers that apart from exposure factors, diverse elimination
21
22
23 323 routes and metabolic fate may exert important roles in determining BPDE-Alb adduct
24
25 324 levels in human serum. Likewise, our results also reveal that BPDE-Alb adducts
26
27
28 325 distribution is not gender specific and there appears to be no correlation with cigarette
29
30
31 326 smoking.

32 327 *4.2 DNA epigenetic alterations in HCC*

33
34
35
36 328 Epidemiology data suggests that increased oxidative stress from chronic hepatitis
37
38
39 329 virus infection and environmental chemical exposures are involved in the
40
41
42 330 pathogenesis of HCC (Li et al., 2013 and Martin and Herceg, 2012). Viral infection
43
44
45 331 and environmental toxicants generate chronic inflammation and induce DNA damage
46
47
48 332 *via* reactive oxygen species (Martin and Herceg, 2012). Oxidative stress has also been
49
50
51 333 reported to interfere with epigenetic mechanisms, which can recruit DNMTs and
52
53 334 Snail-dependent pathway to promoter hypermethylation of several specific gene
54
55
56 335 promoter regions and silence their expression (Hamilton, 2010 and Lim et al., 2008).
57
58
59 336 Such epigenetic alterations might be early events in carcinogenesis and play key roles

1 337 in hepato-carcinogenesis.

2
3 338 We employed HRM analysis, a highly sensitive and specific method for
4
5
6 339 detection and quantification of DNA methylation. HRM technology robustly
7
8
9 340 distinguishes promoter region DNA into fully methylated and heterogeneous status.
10
11 341 The precision of the HRM quantitative approach was tested by BSP analyses, and
12
13
14 342 both results were highly concordant (Figure 2). We observed a high frequency of
15
16
17 343 *GSTP* hypermethylation in the HCC group (53.3%), agreeing with previous studies
18
19
20 344 showing a methylation-associated inactivation of *GSTP* in liver tumours (Lambert et
21
22
23 345 al., 2011, Yang et al., 2003 and Zhang et al., 2005). Additionally, we also found *GSTP*
24
25
26 346 hypermethylation in a few control group participants. A possible explanation for these
27
28
29 347 observations could be that epigenetic alternations are early events in carcinogenesis.
30
31 348 The age factor may also influence DNA methylation modification (Lambert et al.,
32
33
34 349 2011), and all individuals in the cases cohort were slightly older than controls (57.8 vs.
35
36
37 350 57.9 y). We also confirmed in an *in vitro* L02 cell study that *GSTP* expression is
38
39
40 351 silenced due to the promoter region hypermethylation. The π class glutathione
41
42
43 352 *S*-transferase (*GSTP*) is a family of phase II enzymes that can conjugate GSH with
44
45
46 353 various environmental etiological factors. It likely plays important roles in protecting
47
48
49 354 cells against genomic damage mediated by a wide range of oxidants and electrophiles
50
51
52 355 from inflammation and/or environmental exposure (Li et al., 2013 and Zhang et al.,
53
54
55 356 2005). The liver is the major organ for metabolism and detoxification, and silencing
56
57
58 357 *GSTP* expression may result in accumulation of genotoxic agents and elevated
59
60
61 358 oxidative stress, causing DNA damage induction and HCC promotion (Lambert et al.,
62
63
64
65

1 359 2011).

2
3 360 It is noteworthy that herein we focused on cell-free serum DNA, which is easily
4
5
6 361 obtained and a non-invasive measure as opposed to traditional biopsied tumour tissue.
7
8
9 362 Serum and/or plasma samples contain circulating cell-free DNA shed from the
10
11
12 363 primary tumour tissue; this is a ready surrogate for genetic and epigenetic studies
13
14 364 (Huang et al., 2011). DNA methylation modifications in plasma and/or serum samples
15
16
17 365 are highly concordant with those in matched primary tumour specimens (Huang et al.,
18
19
20 366 2011 and Iyer et al., 2010). This study reports similar results for *GSTP*
21
22
23 367 hypermethylation frequency (53.3%) when compared to three previous HCC studies
24
25 368 (54%, 46% and 54%, respectively) (Lambert et al., 2011, Zhang et al., 2005 and Yang
26
27
28 369 et al., 2003).

30 370 *4.3 Association between PAH exposure and GSTP methylation*

31
32
33
34 371 Considering that *GSTP* plays an important role in reactive electrophile
35
36 372 metabolite elimination and antioxidant defence, we further examined the different
37
38
39 373 groups categorized by *GSTP* promoter region methylation status using a stratified
40
41
42 374 analyses. Subjects exhibiting hypermethylation presented with significantly higher
43
44
45 375 PAH-albumin adducts compared to hypomethylated individuals. Additionally, risk of
46
47
48 376 developing HCC was highest amongst individuals who exhibited hypermethylated
49
50
51 377 *GSTP* and elevated burden of BPDE-Alb adducts. These results indicate that *GSTP*
52
53
54 378 plays an important role in PAH detoxification *in vivo*. Previous *in vitro* studies have
55
56 379 also confirmed that *GSTP*-transfected HepG2 cells are more resistant to PAH toxicity.
57
58
59 380 *GSTP* polymorphisms affect such protection, and HepG2 cells transfected with
60
61
62
63
64
65

1 381 insert-free vector acquire high levels of PAH-induced DNA damage *via* formation of
2
3 382 PAH-DNA adducts (Hu et al., 1999). Epidemiology also suggests a significant
4
5
6 383 association between *GSTP* promoter hypermethylation with AFB₁-DNA adducts in
7
8
9 384 HCC (Zhang et al., 2005).

10
11 385 To investigate the *GSTP* protective mechanism against PAH exposure in liver
12
13
14 386 cells, we employed the human liver L02 cell line and DAC-treated L02 cells as an *in*
15
16
17 387 *vitro* model, exposed to low-dose B[a]P (≤ 10 nM). *CYP1A1*, which converts B[a]P
18
19
20 388 into BPDE during phase I biotransformation, was induced by PAH exposure in both
21
22
23 389 cell models. BPDE may then be detoxified by *GSTP* during phase II reactions. *GSTP*
24
25
26 390 can determine BPDE levels, thus influencing resulting genotoxicity. However,
27
28
29 391 detoxification of reactive metabolite was only observed in PAH-induced DAC-treated
30
31
32 392 L02 cells. Our results indicate that *GSTP* hypermethylation results in gene silencing
33
34
35 393 and loss of its protective function. Thus oxidative stress response gene Heme
36
37
38 394 oxygenase-1 (*HO-1*), cell cycle regulation gene (*P53*), DNA methyltransferases genes
39
40
41 395 (*DNMT1*, *DNMT3A* and *DNMT3B*) and DNA mismatch repair genes (*HMLH1* and
42
43
44 396 *HPMS2*) were significantly induced by B[a]P exposure. This infers that *GSTP*
45
46
47 397 promoter region hypermethylation causes failure in catalysing GSH conjugation of
48
49
50 398 BPDE and results in accumulation of PAH-Alb and/or PAH-DNA adducts.

51 399 Herein, selection bias and information bias were stringently controlled for.
52
53 400 Potential confounding factors were ruled out using stratified analysis or multiple
54
55
56 401 factor analysis. There were some limitations in the present study. It is a retrospective
57
58
59 402 case-control epidemiological study, which has its inherent limitations and
60
61
62

1 403 disadvantages. Due to the relatively small sample size, these findings need to be
2
3 404 confirmed in a larger cohort study. Although epidemiological data were complimented
4
5
6 405 with *in vitro* cell models, it remains difficult to identify the exact chronological order
7
8
9 406 for the elevation in BPDE-Alb adducts and the hypermethylation of *GSTP* promoter
10
11
12 407 region. However, environmental PAH exposure and *GSTP* methylation associated
13
14
15 408 with the risk of developing HCC is observed.

16
17 409 In conclusion, we observe that *GSTP* promoter region methylation in
18
19
20 410 circulating-free DNA isolated from serum is positively associated with HCC risk and
21
22
23 411 may serve as an early epigenetic susceptibility biomarker. In addition, there appears to
24
25
26 412 be an associated effect of environmental PAH exposure and *GSTP* methylation on risk
27
28
29 413 of developing HCC. However, the interaction between environmental exposure and
30
31
32 414 epigenetic alteration on HCC risk requires further investigation.

33
34 415

35 36 416 **Acknowledgments**

37
38
39 417 This study was financially supported by National Natural Science Foundation of
40
41
42 418 China 2011 foundation (21177123, 21307126) and the related NSFC-RC International
43
44
45 419 Exchange Programme 2013, the Hundred Talent Program of the Chinese Academy of
46
47
48 420 Sciences (CAS) for 2010 on Human Exposure to Environmental Pollutant and Health
49
50
51 421 Effect, CAS/SAFEA International Partnership Program for Creative Research Teams
52
53
54 422 (KZCX2-YW-T08) and the Xiamen Science and Technology Fund (3502Z20122003).

55
56 423 We thank all who contributed their samples and participated in this study.
57
58
59 424

1 **425 Reference**
2
3

- 4 426 Autrup H, Daneshvar B, Dragsted LO, Gamborg M, Hansen M, Loft S, Okkels H,
5
6 427 Nielsen F, Nielsen PS, Raffn E, Wallin H, Knudsen LE. Biomarkers for exposure to
7
8
9 428 ambient air pollution-comparison of carcinogen-DNA adduct levels with other
10
11 429 exposure markers and markers for oxidative stress. *Environ Health Perspect*. 1999;
12
13
14 430 107(3):233-8.
15
16
17 431 Chen JG, Song XM. An evaluation on incident cases of liver cancer in China. *Bulletin*
18
19
20 432 of *Chinese Cancer* 2005;1:28-31.
21
22
23 433 Chen SY, Wang LY, Lunn RM, Tsai WY, Lee PH, Ahsan H et al. Polycyclic
24
25 434 aromatic hydrocarbon-DNA adducts in liver tissues of hepatocellular carcinoma
26
27
28 435 patients and controls. *Int J Cancer* 2002; 99:14-21.
29
30
31 436 Esteller M, Corn PG, Baylin SB, Herman JG. A gene hypermethylation profile of
32
33
34 437 human cancer. *Cancer Res* 2001;61:3225-3229.
35
36
37 438 Feng Z, Hu W, Chen JX, Pao A, Li H, Rom W, Hung MC, Tang MS. Preferential
38
39 439 DNA damage and poor repair determine ras gene mutational hotspot in human
40
41
42 440 cancer. *J Natl Cancer Inst*. 2002;94(20):1527-36.
43
44
45 441 Hamilton JP. Epigenetic mechanisms involved in the pathogenesis of hepatobiliary
46
47
48 442 malignancies. *Epigenomics*, 2010;2(2):233-243.
49
50
51 443 Herceg Z. Epigenetics and cancer: towards an evaluation of the impact of
52
53 444 environmental and dietary factors. *Mutagenesis* 2007;22:91-103.
54
55
56 445 Hu X, Herzog C, Zimniak P, Singh SV. Differential protection against
57
58 446 benzo[a]pyrene-7,8-dihydrodiol-9,10-epoxide-induced DNA damage in HepG2
59
60
61
62
63
64
65

1 447 cells stably transfected with allelic variants of pi class human glutathione
2
3 448 S-transferase. *Cancer Res.* 1999;59(10):2358-62.
4
5
6 449 Huang ZH, Hu Y, Hua D, Wu YY, Song MX, Cheng ZH. Quantitative analysis of
7
8 450 multiple methylated genes in plasma for the diagnosis and prognosis of
9
10 451 hepatocellular carcinoma. *Exp Mol Pathol* 2011;91:702-707.
11
12
13 452 Islam GA, Greibrokk T, Harvey RG, Ovrebø S. HPLC analysis of
14
15 453 benzo[a]pyrene-albumin adducts in benzo[a]pyrene exposed rats. Detection of
16
17 454 cis-tetraols arising from hydrolysis of adducts of anti- and syn-BPDE-III with
18
19 455 proteins. *Chem Biol Interact* 1999;123:133-148.
20
21
22 456 Iyer P, Zekri AR, Hung CW, Schiefelbein E, Ismail K, Hablas A et al. Concordance of
23
24 457 DNA methylation pattern in plasma and tumor DNA of Egyptian hepatocellular
25
26 458 carcinoma patients. *Exp Mol Pathol* 2010;88:107-111.
27
28
29 459 Johnson N M, Qian G, Xu L, et al. Aflatoxin and PAH exposure biomarkers in a US
30
31 460 population with a high incidence of hepatocellular carcinoma[J]. *Science of the*
32
33 461 *total environment*, 2010;408(23): 6027-6031.
34
35
36 462 Källberg H, Ahlbom A, Lars Alfredsson L. Calculating measures of biological
37
38 463 interaction using R. *Eur J Epidemiol* 2006;21:571-573.
39
40
41 464 Ko CB, Kim SJ, Park C, Kim BR, Shin CH, Choi S, Chung SY, Noh JH, Jeun JH,
42
43 465 Kim NS, Park R. Benzo(a)pyrene-induced apoptotic death of mouse hepatoma
44
45 466 Hepa1c1c7 cells via activation of intrinsic caspase cascade and mitochondrial
46
47 467 dysfunction. *Toxicology* 2004;199(1):35-46.
48
49
50 468 Kumaki Y, Oda M, Okano M. Quantification tool for methylation analysis. *Nucleic*
51
52
53
54
55
56
57
58
59
60
61
62
63
64
65

1 469 Acids Res 2008;36:170-175.
2
3 470 Li T, Zhao XP, Wang LY, Gao S, Zhao J, Fan YC, Wang K. Glutathione S-transferase
4
5
6 471 P1 correlated with oxidative stress in hepatocellular carcinoma Int J Med Sci.
7
8
9 472 2013;10(6):683-90.
10
11 473 Lim SO, Gu, JM, Kim MS, Kim HS, Park YN, Park CK, Cho JW, Park YM, Jung G.
12
13 474 Epigenetic Changes Induced by Reactive Oxygen Species in Hepatocellular
14
15 475 Carcinoma: Methylation of the E-cadherin Promoter. Gastroenterology. 2008;135
16
17 476 (6): 2128-40.
18
19
20 477 Lambert MP, Paliwal A, Vaissière T, Chemin I, Zoulim F, Tommasino M et al.
21
22 478 Aberrant DNA methylation distinguishes hepatocellular carcinoma associated with
23
24 479 HBV and HCV infection and alcohol intake. J Hepatol 2011;54:705-715.
25
26
27 480 Martin M, Herceg Z. From hepatitis to hepatocellular carcinoma: a proposed model
28
29 481 for cross-talk between inflammation and epigenetic mechanisms. Genome medicine
30
31 482 2012;4(1):8.
32
33
34 483 Niu JJ, Su YH, Han YF, Zhao R, Sun XL, Guo F et al. Synergistic effects of different
35
36 484 types of smoking and other risk factors on risk of hepatocellular carcinoma in
37
38 485 Xiamen, China. Chin J Epidemiol 2010;31:850-855.
39
40
41 486 Parkin DM, Bray F, Ferlay J, Pisani P. Global cancer statistics. CA Cancer J Clin
42
43 487 2002;55:74-108.
44
45
46 488 Stanzer S, Balic M, Strutz J, Heitzer E, Obermair F, Hauser-Kronberger C, et al.
47
48 489 Rapid and reliable detection of LINE-1 hypomethylation using high-resolution
49
50 490 melting analysis. Clin Biochem 2010;43:1443-1448.
51
52
53
54
55
56
57
58
59
60
61
62
63
64
65

1 491 Su Y, Zhao B, Guo F, Bin Z, Yang Y, Liu S, Han Y, Niu J, Ke X, Wang N, Geng X, Jin
2
3 492 C, Dai Y, Lin Y. Interaction of benzo[a]pyrene with other risk factors in
4
5
6 493 hepatocellular carcinoma: a case-control study in Xiamen, China. *Annals of*
7
8
9 494 *epidemiology* 2014;24(2):98-103
10
11 495 Tang WY, Levin L, Talaska G, Cheung YY, Herbstman J, Tang D et al. Maternal
12
13 496 exposure to polycyclic aromatic hydrocarbons and 5'-CpG methylation of
14
15
16
17 497 interferon- γ in cord white blood cells. *Environ Health Perspect*
18
19
20 498 2012;120:1195-1200.
21
22 499 Tian M, Peng S, Martin FL, Zhang J, Liu L, Wang Z et al. Perfluorooctanoic acid
23
24
25 500 induces gene promoter hypermethylation of glutathione-S-transferase Pi in human
26
27
28 501 liver L02 cells. *Toxicology* 2012;296:48-55.
29
30
31 502 Wu HC, Wang Q, Wang LW, Yang HI, Ahsan H, Tsai WY, Wang LY, Chen SY, Chen
32
33
34 503 CJ, Santella RM. Polycyclic aromatic hydrocarbon- and aflatoxin-albumin adducts,
35
36
37 504 hepatitis B virus infection and hepatocellular carcinoma in Taiwan. *Cancer Lett.*
38
39
40 505 2007;252(1):104-14.
41
42 506 Xu XF, Cai L, Dai L, Kang TC, Chen SQ. Mortality analysis and the tendency
43
44
45 507 prediction of cancer in Tongan District, Fujian. *Strait J Prev Med Methods*
46
47
48 508 2003;9:14-16.
49
50 509 Yang B, Guo M, Herman JG, Clark DP. Aberrant promoter methylation profiles of
51
52
53 510 tumor suppressor genes in hepatocellular carcinoma. *Am J Pathol*
54
55
56 511 2003;163:1101-7.
57
58 512 Zhang YJ, Chen Y, Ahsan H, Lunn RM, Chen SY, Lee PH, Chen CJ, Santella RM.

1 513 Silencing of glutathione S-transferase P1 by promoter hypermethylation and its
2
3 514 relationship to environmental chemical carcinogens in hepatocellular carcinoma.
4
5
6 515 Cancer Lett. 2005;221(2):135-43.
7
8
9 516 Zhang YJ, Wu HC, Shen J, Ahsan H, Tsai WY, Yang HI et al. Predicting
10
11 517 hepatocellular carcinoma by detection of aberrant promoter methylation in serum
12
13
14 518 DNA. Clin Cancer Res 2007;13:2378-2384.
15
16
17 519 Zhao B, Shen H, Liu F, Liu S, Liu J, Guo F, Sun X. Exposure to organochlorine
18
19
20 520 pesticides is independent risk factor of hepatocellular carcinoma: a case-control
21
22
23 521 study. J Expo Sci Environ Epidemiol 2012;21:601-608.
24
25
26 522 Zhao BH, Guo F, Liu S, Pan LL. The study on the interactions between polycyclic
27
28 523 aromatic hydrocarbon-albumin adducts and various risk factors to primary
29
30
31 524 hepatocellular carcinoma. Chin J Prev Med 2010;44:427-432.
32
33
34 525
35
36 526
37
38
39 527
40
41
42 528
43
44
45 529
46
47
48 530
49
50
51 531
52
53 532
54
55
56 533
57
58
59 534
60
61
62
63
64
65

1 535 **Figure Legends**

2
3 536

4
5
6 537 **Figure 1. High resolution melting assay using serial dilution of methylated**
7
8
9 538 **plasmid DNA (from 100% to 0%).** (A) High resolution melting curve of standard
10
11
12 539 serial dilutions of methylated *GSTP* promoter region; and, (B) values of relative
13
14
15 540 signal were plotted against the percentage of methylation for each dilution to generate
16
17 541 a typical standard curve. All the experiments were performed in duplicate.

18
19
20 542
21
22 543
23
24
25 544 **Figure 2. High resolution melting (HRM) and bisulfite sequencing PCR (BSP)**

26
27
28 545 **analysis of *GSTP* promoter status in representative serum samples.** (A) HRM
29
30
31 546 curve of *GSTP* promoter methylated standard (red), unmethylated standard (green),
32
33
34 547 unmethylated serum (black), methylated serum (yellow), fully methylated serum (blue)
35
36 548 and heterozygous methylated serum (purple); (B) Representative BSP analysis of
37
38
39 549 *GSTP* promoter fully methylated serum; (C) Representative BSP analysis of *GSTP*
40
41
42 550 promoter unmethylated serum; (D) Representative BSP analysis of *GSTP* promoter
43
44
45 551 methylated serum; and, (E) Representative BSP analysis of *GSTP* promoter
46
47
48 552 heterozygous methylated serum. In B-E, each line represents one DNA strand; the
49
50
51 553 numbers at the top of the parallel line identify the location of the cytosine at the CpG
52
53
54 554 sites; the open circles are unmethylated CpGs; the filled-in circles are methylated
55
56 555 CpGs.

57
58 556
59
60
61
62
63
64
65

1 557 **Figure 3. Distribution BPDE-Alb exposure level in *GSTP* promoter unmethylated,**
2
3 558 **heterozygous and methylated groups.** All individual divided into unmethylated,
4
5
6 559 heterozygous and methylated groups. Bar indicates media, *P* for Mann-Whitney test.
7
8

9 560
10
11 561 **Figure 4. RT-PCR and BSP analysis of *GSTP* expression and methylation in A549**
12
13 562 **cells, DAC-treated A549 cells, L02 cells and DAC-treated L02 cells.** (A) *GAPDH*
14
15 563 as internal reference. *GSTP* is normally expressed in A549 cells, silenced in L02 cells
16
17 564 but is restored upon DAC treatment; (B) The CpG methylation rates (%) for *GSTP*
18
19 565 CpGs -226 to +84 in the control and DAC-treated groups for A549 and L02 are
20
21 566 shown, DAC significantly decreased *GSTP* promoter methylation levels and restored
22
23 567 *GSTP* mRNA expression in L02 cells.
24
25
26
27
28
29
30
31
32

33 569 **Figure 5. BSP analysis of DAC-treated L02 cell *GSTP* promoter methylation**
34
35 570 **status in response to 24 h different dose of B[a]P exposure.** The CpG methylation
36
37 571 rates (%) for *GSTP* promoter -226 to +84 in the DMSO control groups $61.6 \pm 9.9\%$
38
39 572 (A); 0.1 nM B[a]P groups $65.5 \pm 8.7\%$ (B); 1 nM B[a]P groups $61.1 \pm 12.1\%$ (C); and,
40
41 573 10 nM B[a]P groups $60.3 \pm 10.7\%$ (D). L02 cells were treated with 5 μ M
42
43 574 5-aza-2'-deoxycytidine (DAC) for 2 days prior to exposure, and then exposed to 0.1, 1,
44
45 575 10 nM B[a]P or with DMSO alone (vehicle). In A-D, each line represents one DNA
46
47 576 strand; the numbers at the top of the parallel line identify the location of the cytosine
48
49 577 at the CpG sites. The open circles are unmethylated CpGs the filled-in circles are
50
51 578 methylated CpGs.
52
53
54
55
56
57
58
59
60
61
62
63
64
65

1 579 **Figure 6. Real-time RT-PCR analysis of gene expression in L02 cells (A) and**
2
3
4 580 **DAC-treated L02 cells (B) in response to B[a]P exposure.** Asterisks (*) indicate
5
6 581 significant difference ($P < 0.05$) when compared to the control. Standard deviation is
7
8
9 582 showed as the error bars, which arise from triplicate tests for all the four independent
10
11
12 583 experiments.
13
14 584

Table1. Sequence of primers used for HRM, quantitative RT-PCR and BSP analysias

Gene	Application	Primer sequence (5'-3')	Product size (bp)	CpG No.
<i>GSTP</i>	HRM/BSP	F: GGGATTTGGGAAAGAGGGAAAGG R: ACCGCTCTTCTAAAAAATCCC	149	17
<i>GSTP</i>	BSP	F: GGGATTTGGGAAAGAGGGAAAGG R: CCCATACTAAAACTCTAAACCCC	311	38
<i>CYP1A1</i>	Q-PCR	F: CATCCCCACAGCACAACA R: CAGGGGTGAGAAACCGTTCA	152	-
<i>GSTP</i>	Q-PCR	F: CGGAGACCTCACCCTGTA R: CGCCTCATAGTTGGTGTAGA	169	-
<i>P53</i>	Q-PCR	F: TCTTCTGTCCCTTCCCAGAA R: AATCAACCCACAGCTGCAC	163	-
<i>DNMT1</i>	Q-PCR	F: TACCTGGACGACCCTGACCTC R: CGTTGGCATCAAAGATGGACA	103	-
<i>DNMT3A</i>	Q-PCR	F: TATTGATGAGCGCACAAGAGAGC R: GGGTGTTCAGGGTAACATTGAG	111	-
<i>DNMT3B</i>	Q-PCR	F: GGCAAGTTCTCCGAGGTCTCTG R: TGGTACATGGCTTTTCGATAGGA	113	-
<i>HMLH1</i>	Q-PCR	F: TCTCAGGCCAGCAGAGTGAA R: TGTGTGAGCGCAAGGCTTTA	93	-
<i>HMSH2</i>	Q-PCR	F: AATGACTTGGAAAAGAAGATGC R: TTAAAGAAGTCAATTTGCTGTTG	223	-
<i>HPMS2</i>	Q-PCR	F: GCACTGAGCGATGTCACCATT R: TTCCTTATGGCGCACAGGTAGT	171	-
<i>GAPDH</i>	Q-PCR	F: GGAGAAGGCTGGGGCTCAT R: TGATGGCATGGACTGTGGTC	230	-

Table2. Demographics and clinical characteristics in cases (n=90) and controls (n=99)

	Characteristic	Case (%)	Control (%)	χ^2 (<i>P</i> -value)
General	Sex			
	Male	76 (84.4)	60 (60.6)	13.3 (<0.001)
	Female	14 (15.6)	39 (39.4)	
	Age (year)			
	<50	46 (51.1)	52 (52.5)	0.04 (0.85)
	≥50	44 (48.9)	47 (47.5)	
	BMI (kg/m ²)			
<24	74 (82.2)	70 (70.7)	3.5 (0.06)	
≥24	16 (17.8)	29 (29.3)		
Life style	Smoking status			
	Non-smoking	40 (44.4)	63 (63.6)	8.4 (0.02)
	Smoking	48 (53.3)	36 (36.3)	
	Missing	2 (2.2)		
	Alcohol consumption			
	None	56 (62.2)	75 (75.8)	11.8 (0.03)
	Drinker	32 (35.6)	24 (24.2)	
Missing	2 (2.2)			
Virus infection and disease	HBV			
	HBV(-)	51 (56.7)	90 (90.9)	29.2 (<0.001)
	HBV (+)	39 (43.3)	9 (9.1)	
	HCV			
	HCV (-)	50 (55.6)	78 (78.8)	11.3 (<0.001)
	HCV (+)	40 (44.4)	21 (21.2)	
	Liver cirrhosis			
	Cirrhosis (-)	72 (81.1)	99 (100)	20.8 (<0.001)
	Cirrhosis (+)	17 (18.9)	0 (0)	
Gene promoter methylation	Methylation status			
	<i>GSTP</i> -U ^a	40 (44.4)	77 (77.8)	35.2 (<0.001)
	<i>GSTP</i> -H ^a	10 (11.1)	11 (11.1)	
	<i>GSTP</i> -M ^a	38 (42.2)	6 (6.1)	
	Missing	2 (2.2)	5 (5.0)	

GSTP methylation status was qualitatively determined by HRM PCR.

^aM, fully methylated; H, heterogeneous; U, fully unmethylated.

Table3. Serum pollutant concentrations and DNA methylation levels in the participants

Characteristic	Case			Control			<i>P</i>
	Mean	SD	Median	Mean	SD	Median	
BPDE-Alb (fmol/mg adduct)	17.71	21.64	1.79	6.48	11.10	1.51	< 0.001
<i>GSTP</i> (%)	12.79	23.38	1.62	2.17	11.16	0.00	< 0.001

Variable distributions were analysed by the nonparametric Mann-Whitney *U*-test.

Table4. Multivariate logistic regression analysis of the interactions of *GSTP* epigenetic vs benzo[a]pyrene exposure in HCC risks

		Case	Control	Crude OR (95% CI)	AOR ^a (95% CI)
<u><i>GSTP</i></u>	<u>BPDE-Alb</u>				
<i>GSTP</i> -U	Low	15	41	1.0 (reference)	1.0 (reference)
<i>GSTP</i> -U	High	24	36	1.1 (0.3-3.3)	1.1 (0.3-4.3)
<i>GSTP</i> -H/M	Low	19	7	4.4 (1.8-10.5)	3.8 (1.3-10.9)
<i>GSTP</i> -H/M	High	29	10	7.7 (3.0-19.6)	8.4 (2.7-26.6)
				<i>P</i> -trend < 0.001	<i>P</i> -trend < 0.001

AOR was adjusted for age, BMI, sex, alcohol consumption, smoking, HBV, HCV, liver cirrhosis each other.

Figure1

[Click here to download high resolution image](#)

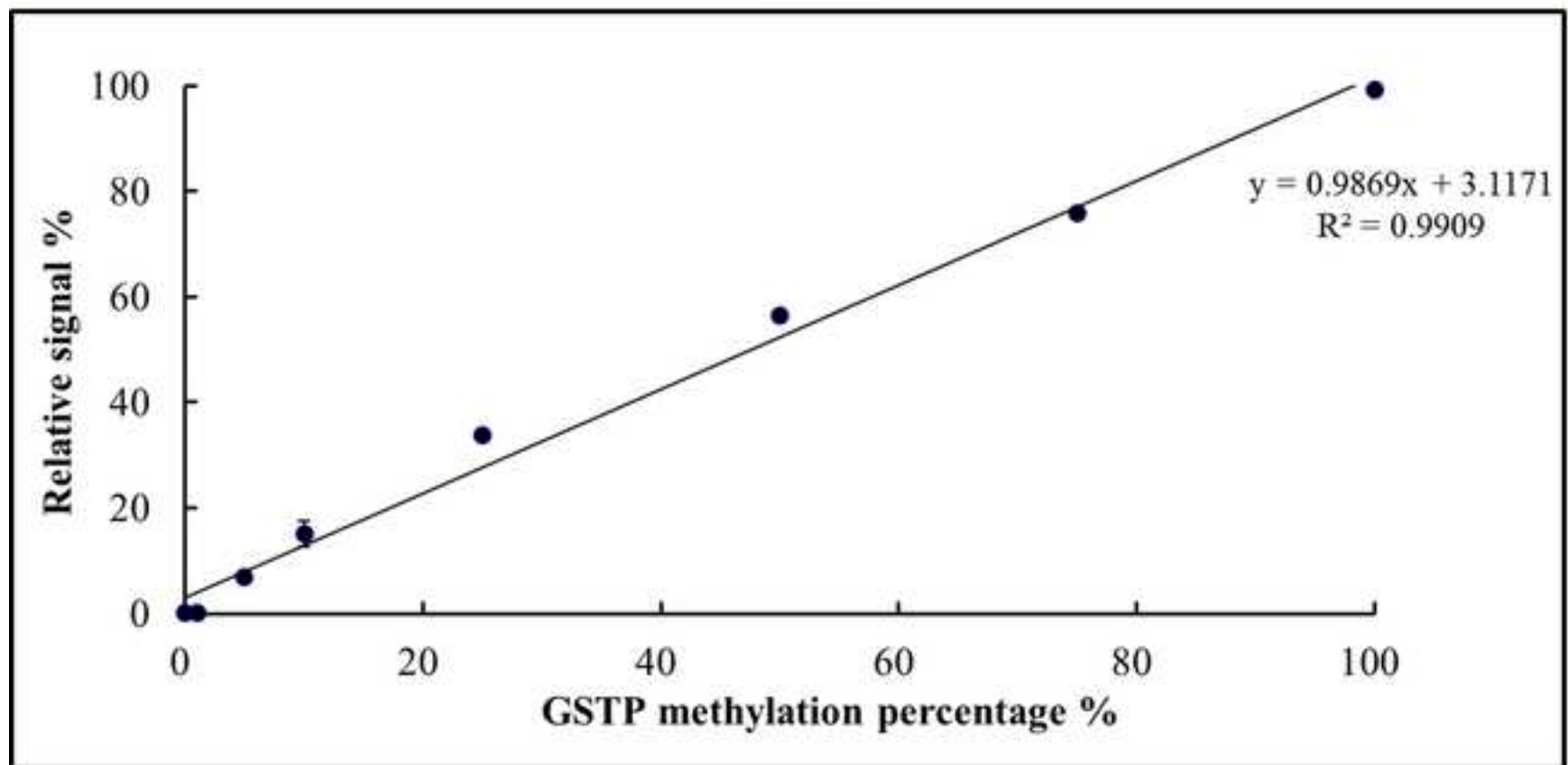
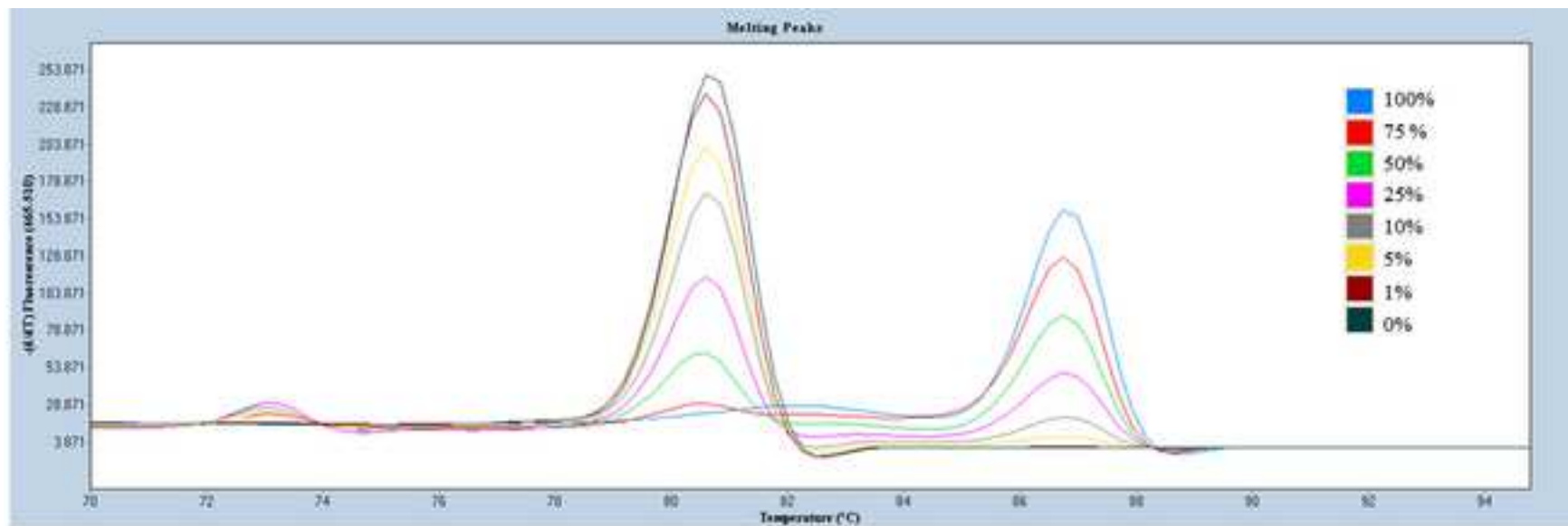


Figure2

[Click here to download high resolution image](#)

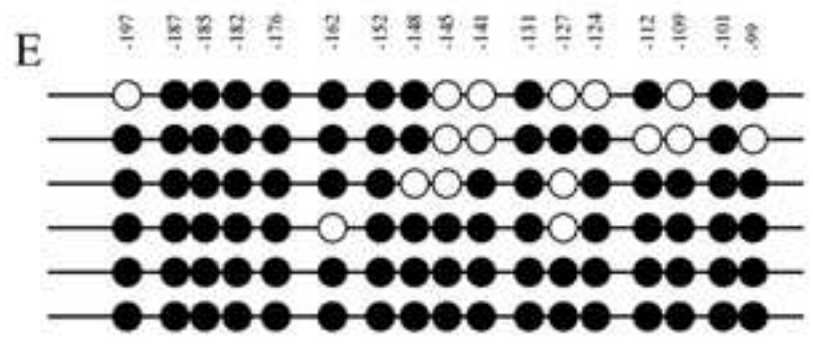
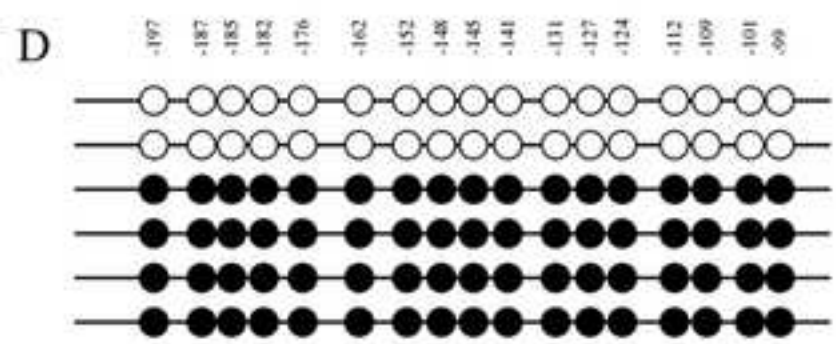
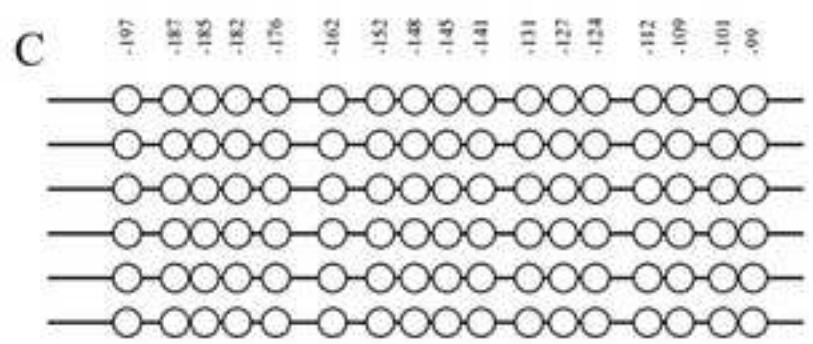
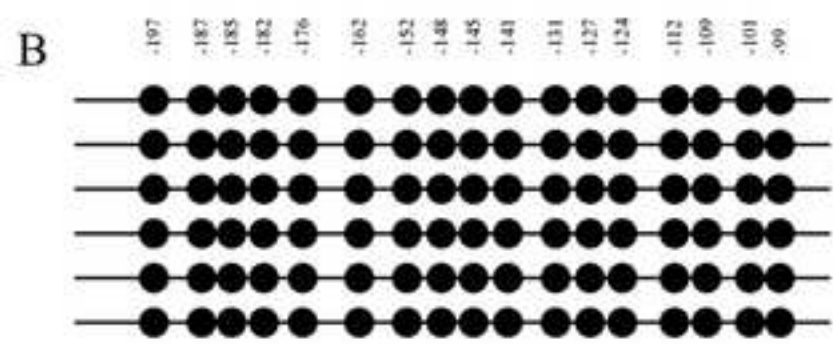
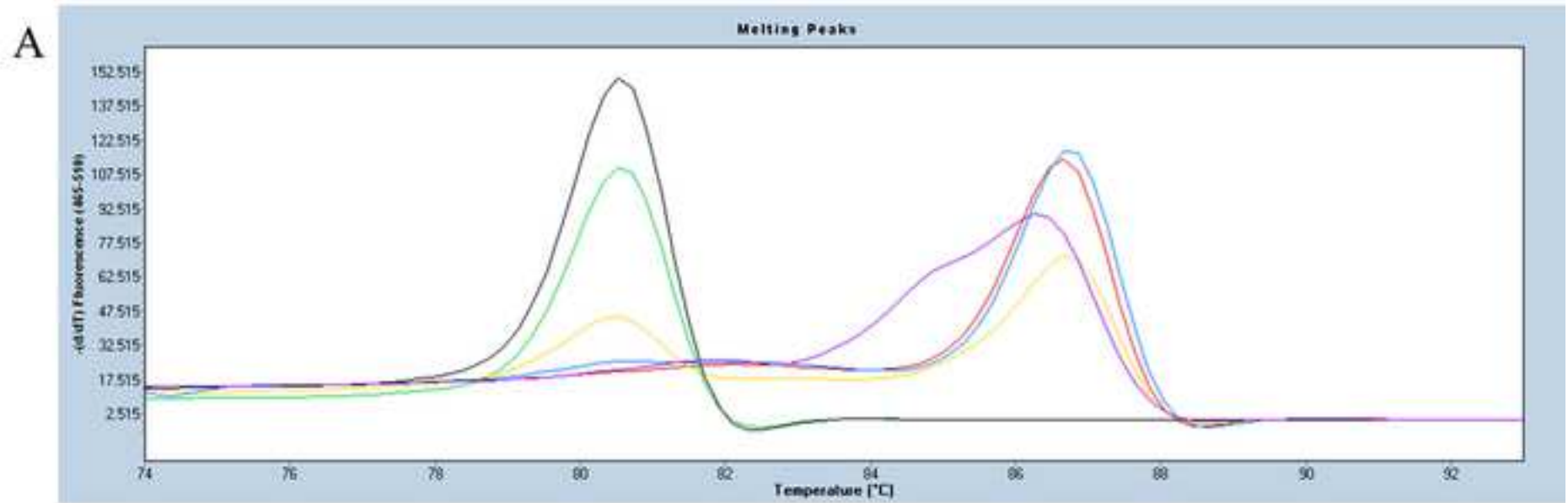


Figure3

[Click here to download high resolution image](#)

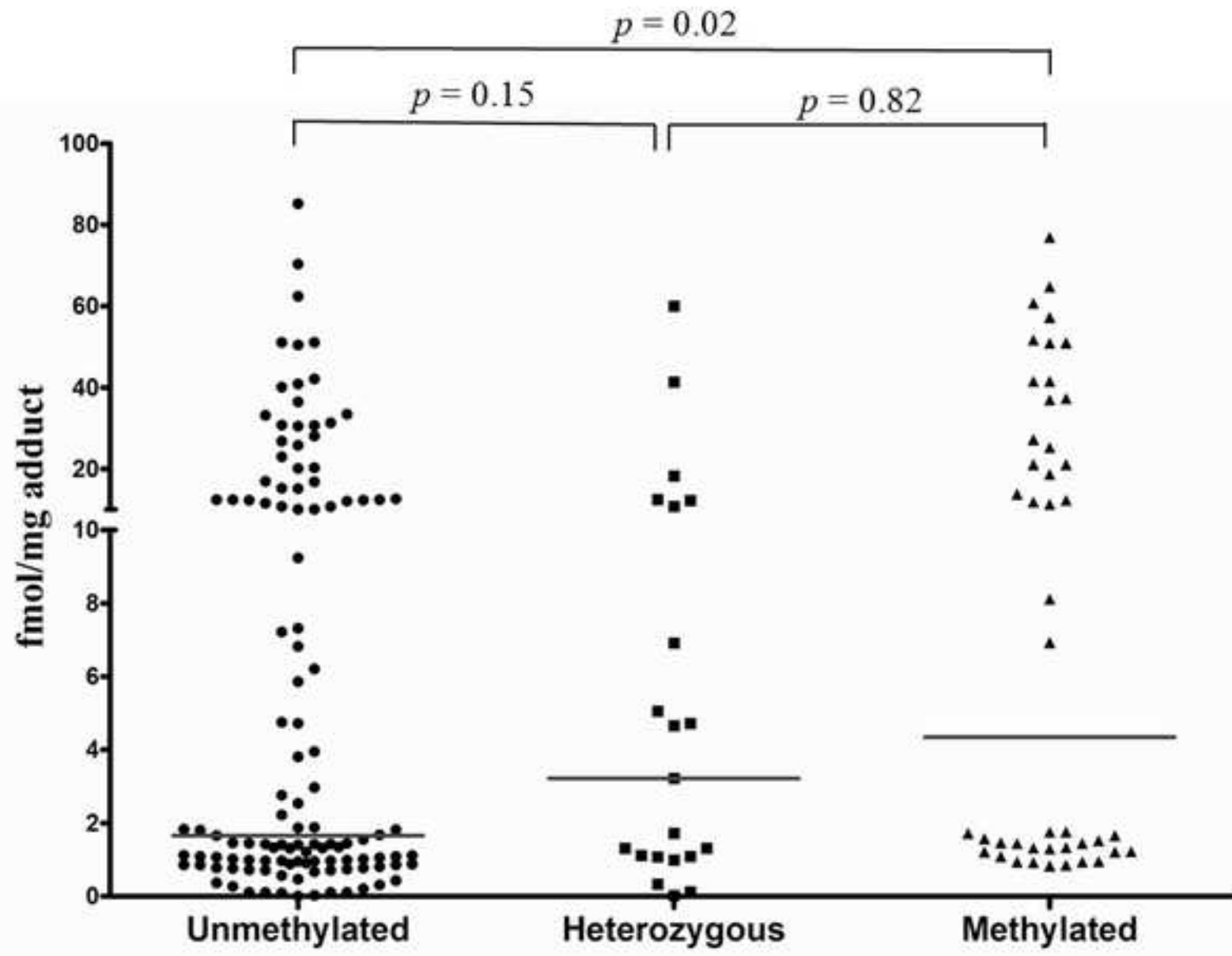


Figure4
[Click here to download high resolution image](#)

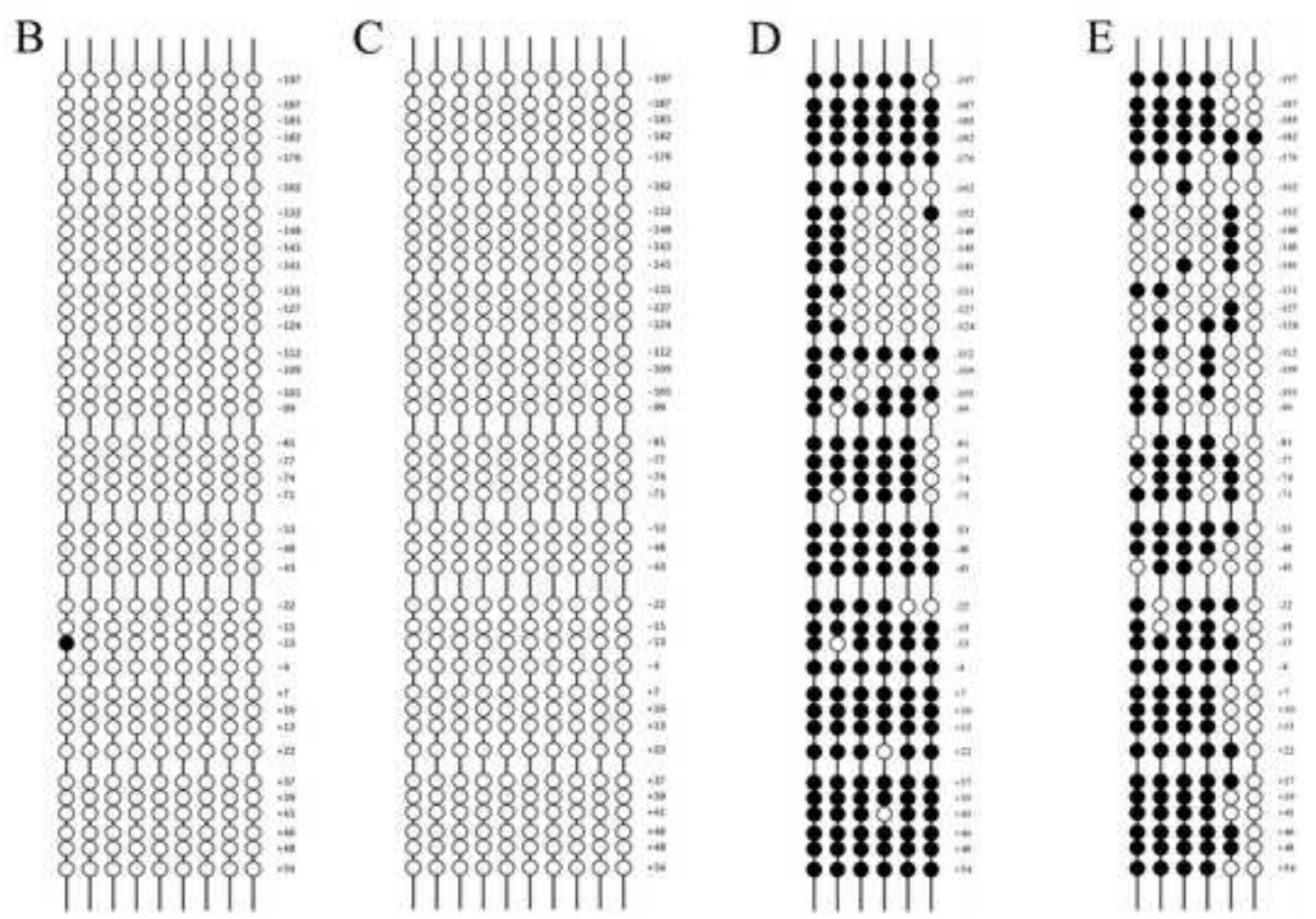
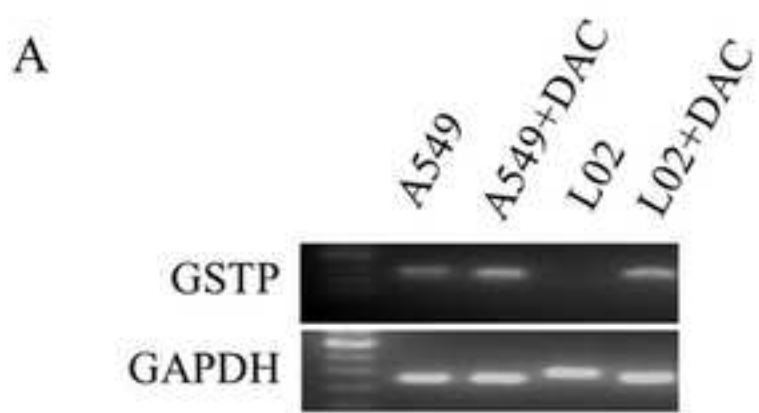


Figure5

[Click here to download high resolution image](#)

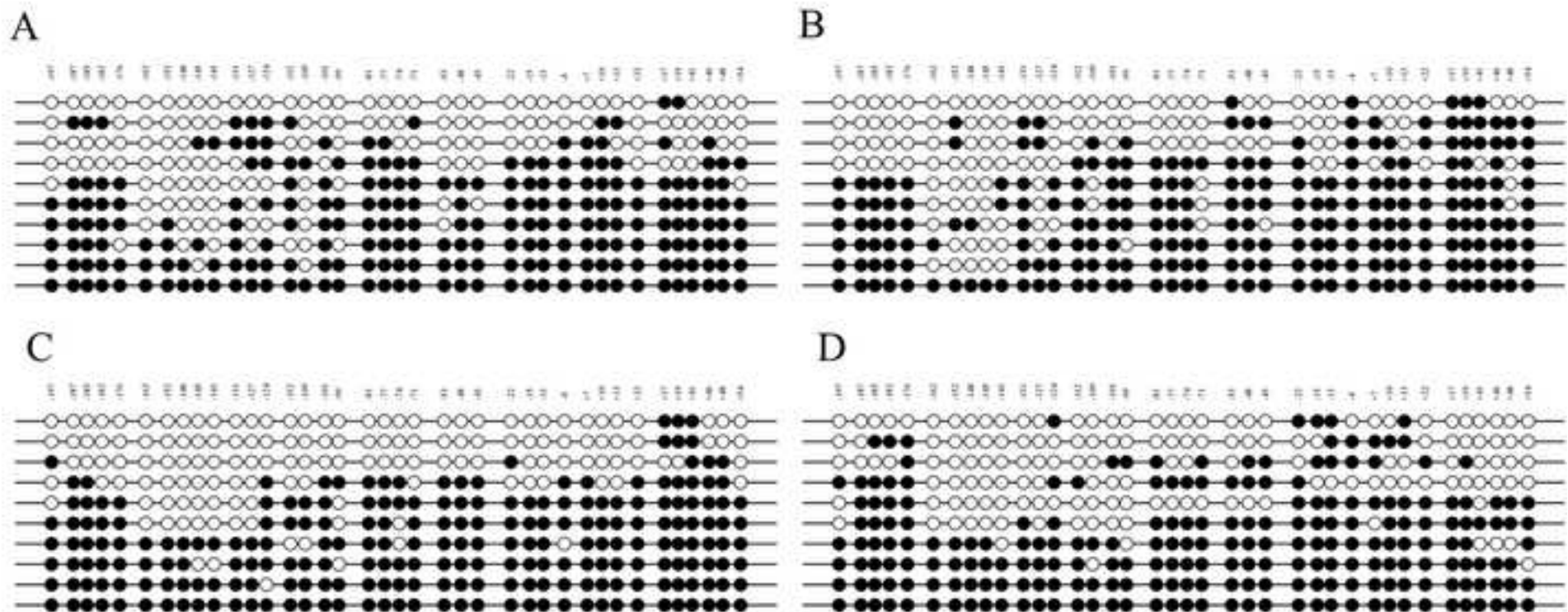


Figure6

[Click here to download high resolution image](#)

